Proposed Mechanism of 1,1-Diamino-Dinitroethylene Decomposition: A Density Functional Theory Study

Asta Gindulytė and Lou Massa

Department of Chemistry, Hunter College, 695 Park Avenue, New York, New York 10021, and
The Graduate School, City University of New York, 33 West 42nd Street, New York, New York 10036

Lulu Huang[†] and Jerome Karle*

*Laboratory for the Structure of Matter, Naval Research Laboratory, Washington, D.C. 20375*

We have investigated the heretofore unknown unimolecular decomposition pathway of the explosive molecule diaminodinitroethylene (DADNE). With the use of DFT methods, whose accuracy has been calibrated by means of ab initio calculations (MP2, MP4, G2) on a simpler but related molecule, nitroethylene, we have been able to characterize the entire decomposition reaction pathway. Importantly, we find that the reaction is initiated by a nitro-to-nitrite rearrangement with a calculated energy barrier of magnitude 59.1 kcal/mol obtained by use of B3LYP (59.7 kcal/mol B3P86) which is very close to the experimental activation energy of 58 kcal/mol. We have been able to characterize every step in the decomposition reaction path leading to fragments NO, HONO, CO, NH_2, and HNC. These may interact to yield final stable products, CO, N_2, H_2O with an energy release that on average is adequate to initiate two additional DADNE molecular decompositions, and thus, sustain a chain reaction. The structural parameters we have calculated for DADNE are consistent with the known experimental crystallographic structure, and also with previous theoretical calculations. Additionally, we have obtained the structural parameters of the initial transition state, as well as each subsequent step along the decomposition pathway. Thus we consider the unimolecular decomposition of DADNE to be well characterized.

Introduction

There have been several recent studies of 1,1-diamino-dinitro-ethylene (DADNE), **A**. The synthesis has been reported[1] and the crystal structure has been determined.[2,3] Its features as an explosive, including the activation energy, have been characterized experimentally.[4] The important properties such as $C-NO_2$ and $C-NH_2$ bond dissociation energies, heats of formation, vaporization, and sublimation have been calculated at the B3P86/6-31G+(d,p) level.[5] As Politzer et al.[5] have pointed out, this compound has the same molecular stoichiometry as RDX, **B**, and HMX, **C**, which are among the most effective currently used explosives and monopropellants, and, upon complete decomposition to CO, N_2, and H_2O, all of these molecules would yield the same high value, 0.0405, for moles of gaseous product per gram of compound, one of the key determinants of explosive and propellant performance. It is interesting to note that the reported activation energy (E_a = 58 kcal/mol for temperature interval 210−250 °C)[4] for DADNE is higher than that of RDX ($E_a \sim$ 40 kcal/mol)[6−8] and HMX ($E_a \sim$ 35 kcal/mol),[9] which favors DADNE as an explosive.

An understanding of the decomposition mechanism, however, also plays a key role in the evaluation of an explosive. The decomposition mechanism for DADNE can be expected to be quite different from that for RDX and HMX. Note that even though DADNE does have the same stoichiometry as RDX and HMX, structurally it bears no similarity to these molecules. Thus, possible reaction pathways involving unimolecular decomposition of these compounds would differ from those studied

A   **B**   **C**
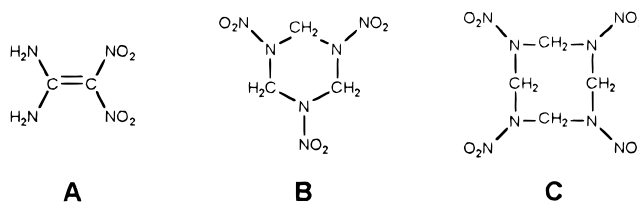
in DADNE. Instead of $C-NO_2$, $N-NO_2$ bond dissociation would occur, and the ring geometries would present the possibility of symmetric ring fission. Theoretical work investigating possible reaction pathways for RDX and HMX has been carried out.[7,8,10−12] Considerable experimental work has been performed with RDX and HMX in order to determine possible decomposition pathways and their relative importance.[13−17]

In this investigation of the decomposition mechanism of DADNE, we have focused on discovering the lowest energy decomposition pathway for unimolecular decomposition of this compound. We have considered the behavior of the nitro group in nitroethylene to be a possible model for the behavior of nitro groups in DADNE, because in both cases a nitro group is adjacent to a carbon−carbon double bond. We employed reasonably inexpensive DFT methods with a moderate size basis set to obtain a qualitative description of the energetic profile for this DADNE decomposition pathway. In nitroethylene, we studied[18] the effect of basis set size on relative energies. It has been found that DFT methods (especially those based upon the Becke three-parameter hybrid (B3) exchange functional) with a moderate basis set yielded good geometries.[19] For a given geometry, a way to obtain a more accurate evaluation of energy values is to carry out a single-point calculation with a larger

† Permanent address: Geo-Centers, Inc., 10903 Indian Head Highway, Fort Washington, MD 20744.

TABLE 1: Total Energies for DADNE, the Two Radicals Resulting from the C$-$NO$_2$ Bond Dissociation and Estimated Bond Dissociation Energy (BDE) for This Bond

	B3P86		B3LYP			BDE, kcal/mol	
structure	energy, a.u.	ZPVE, kcal/mol	energy, a.u.	ZPVE, kcal/mol	method of BDE calculation	B3P86	B3LYP
$(H_2N)_2C\!\!=\!\!C(NO_2)_2$	-599.70979	58.23	-598.35631	57.68	uncorrected for ZPVE	73.1	67.1
$(H_2N)_2C\!\!=\!\!\overset{\bullet}{C}(NO_2)$	-394.10864	48.29	-393.16541	47.80	corrected for unscaled ZPVE	68.8	62.8
$\bullet NO_2$	-205.48464	5.65	-205.08389	5.51	corrected for scaled ZPVE	68.9	62.9

basis set. In the case of nitroethylene, however, we found that larger basis sets did not significantly improve the energy values obtained with the moderate basis set used here. In our nitroethylene study we employed the ab initio methods MP2, MP4, and also G2, which are expected to give highly accurate energy values, as well as DFT methods based upon B3 exchange and two different correlation energy functionals, viz., LYP and P86. In most decomposition steps, LYP performed better than P86, except for estimations of bond dissociation energies (BDE), as judged by comparison with ab initio results. With DADNE, we also applied both B3LYP and B3P86 to get a sense of the variability associated with different correlation energy functionals. We found that, while there are some quantitative differences between DFT and ab initio results, the qualitative trends are the same. Furthermore, we anticipated that the DFT error estimates (measured against G2 as a standard) obtained for nitroethylene might be applied to DADNE for those particular steps in the decomposition pathway which are essentially the same.

Computational Details

All quantum mechanical calculations were performed with the *Gaussian 98* program package.[20] The reader is referred to ref 21 for definitions of technical symbols. The Becke three-parameter hybrid (B3)[22] was used in conjunction with two correlation functional methods. The functionals were the Perdew-86 (P86)[23] and the Lee$-$Yang$-$Parr (LYP).[24] For all calculations, a Gaussian-type basis set, 6-31+G(d,p) was used. Thus, geometries of all reactants, products, and transition states were optimized by the use of the two methods, B3P86/6-31+G-(d,p) and B3LYP/6-31+G(d,p). Default convergence criteria were used for all structures except structure **9**. In that case, default criteria for B3LYP gave a small negative frequency. Upon tightening the convergence criteria, the negative frequency disappeared. Vibrational frequencies were calculated with the use of the same approximation for characterization of the nature of stationary points and zero-point vibrational energy (ZPVE) corrections. All of the stationary points have been positively identified for minimum energy with no imaginary frequencies and the transition states with one imaginary frequency. For anharmonicity correction,[25] the calculated ZPVE values were scaled by 0.9759 and by 0.9806 for B3P86 and B3LYP calculations, respectively. Intrinsic reaction coordinate (IRC) analysis was carried out for each transition state to make sure that it is the transition structure connecting the desired reactants and products. For all structures with an even number of electrons, a restricted (doubly occupied orbitals) wave function was used. For the high-energy structure, transition state [**2**]†, however, an unrestricted wave function was also implemented to check the result. For all doublet structures an unrestricted wave function was used and examined for spin contamination, which was found to be inconsequential.

Results and Discussion

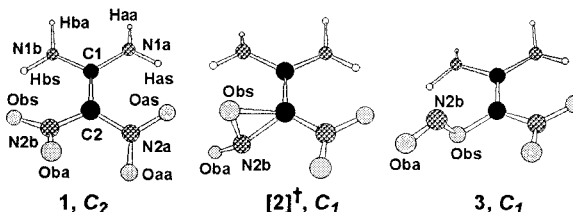**Initial Step of DADNE Decomposition.** The initial step in thermal decomposition of nitro-containing compounds is often

the cleavage of a C$-$NO$_2$ or N$-$NO$_2$ bond.[26] The C$-$NH$_2$ bond is known to have a very high bond dissociation energy.[5] Therefore, we calculated the C$-$NO$_2$ bond dissociation energy (BDE) for DADNE. The results are displayed in Table 1. Our B3P86 value of 68.9 kcal/mol is consistent with the result obtained by Politzer et al.[5] by use of the same method. The BDE obtained with B3LYP is 62.9 kcal/mol. Both of these values may be underestimates. Our previous study of nitroethylene[18] showed that B3LYP and B3P86 underestimate the C$-$NO$_2$ bond dissociation energy for nitroethylene by $\sim$8 and $\sim$4 kcal/mol respectively, as compared to the G2 result. We thus predict that the BDE for DADNE should probably be around 73 kcal/mol, which is quite high compared to the experimental E_a of 58 kcal/mol,[4] and therefore there must exist a lower energy process which is responsible for the initial decomposition step of this molecule.

We previously found that nitro-to-nitrite rearrangement is the lowest energy decomposition pathway ($\sim$15 kcal/mol lower than the C$-$NO$_2$ bond cleavage) for nitroethylene.[18] Investigation of the nitro-to-nitrite rearrangement in DADNE verified that the same is true for this molecule. The barrier for the rearrangement is 59.7 and 59.1 kcal/mol, as obtained with B3P86 and B3LYP methods, respectively. Furthermore, based on our investigation of the same reaction for nitroethylene, for which G2, B3LYP and B3P86 results agree very closely, we argue that the error of this calculation should be rather small. Note that this result compares very well to the experimental activation energy (E_a) of 58 kcal/mol.[4]

The structures and optimized geometrical parameters for DADNE, **1**, the transition state, [**2**]†, and the isonitrite product, **3**, are shown in Table 2. Note that DADNE is not a planar structure. Because of the repulsion between the two NO$_2$ groups, they are rotated by more than 20° with respect to the C1$-$C2$-$N plane. When further rotation of either NO$_2$ group occurs, a possibility of C$-$O bond formation and thus nitro-to-nitrite rearrangement emerges. In the transition state structure, [**2**]†, the C2$-$N2b bond is elongated to 1.536 Å from that of 1.432 Å in DADNE, and a new C2$-$Obs bond of 1.785 Å is formed. Upon formation of the product, isonitrite, **3**, the C2$-$N2b bond is broken, and the C2$-$Obs bond shortens to 1.355 Å. To avoid confusion, we mention in passing that both Obs and Oba are equally capable of forming the bond with C2. IRC analysis of [**2**]† led to a reactant with the NO$_2$ group rotated perpendicularly to the C1$-$C2$-$N2 plane, and this group can subsequently rotate either way.

We now proceed with a description of the DADNE decomposition steps following the nitro-to-nitrite rearrangement. Figure 1 provides a scheme of unimolecular DADNE decomposition, via the nitro-to-nitrite rearrangement pathway, through formation of small fragments, which can further react among themselves to form stable products, such as CO, N$_2$, and H$_2$O. In addition, the structures and optimized geometrical parameters of species **7**$-$**17** are also shown in Figure 1, while the structures and optimized geometrical parameters for species **1**$-$**3** and **4**$-$**6** are displayed in Table 2 and Table 3, respectively. Table 4 lists the calculated energies of all chemical species involved in the

1,1-Diamino-Dinitroethylene Decomposition

J. Phys. Chem. A, Vol. 103, No. 50, 1999 **11047**

TABLE 2: Selected Structural Parameters for Species 1−3

1, C_2 [2]†, C_1 3, C_1
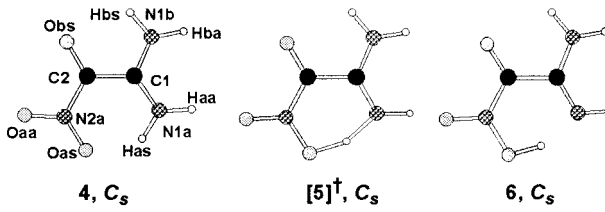
Geometrical Parameter	1 B3P86	1 B3LYP	2 B3P86	2 B3LYP	3 B3P86	3 B3LYP
C(1)-C(2)a	1.426	1.428	1.419	1.422	1.395	1.399
C(1)-N(1a)	1.339	1.345	1.341	1.347	1.345	1.350
C(1)-N(1b)	1.339	1.345	1.347	1.352	1.363	1.369
C(2)-N(2a)	1.424	1.432	1.405	1.410	1.400	1.409
C(2)-N(2b)	1.424	1.432	1.515	1.536	—	—
C(2)-O(bs)	—	—	1.766	1.785	1.354	1.355
N(1a)-H(aa)	1.007	1.008	1.007	1.009	1.007	1.009
N(1a)-H(as)	1.019	1.017	1.019	1.018	1.019	1.018
N(1b)-H(ba)	1.007	1.008	1.009	1.011	1.009	1.010
N(1b)-H(bs)	1.019	1.017	1.014	1.014	1.010	1.011
N(2a)-O(aa)	1.219	1.225	1.225	1.231	1.231	1.238
N(2a)-O(as)	1.251	1.257	1.255	1.262	1.256	1.263
N(2b)-O(ba)	1.219	1.225	1.227	1.232	1.155	1.154
N(2b)-O(bs)	1.251	1.257	1.341	1.350	1.536	1.583
C(2)-C(1)-N(1a)b	121.1	121.3	121.5	121.7	123.9	124.3
C(2)-C(1)-N(1b)	121.1	121.3	119.3	119.6	118.0	118.0
N(1a)-C(1)-N(1b)	117.8	117.3	119.0	118.5	118.2	117.7
C(1)-C(2)-N(2a)	121.6	121.7	124.5	124.9	123.8	123.7
C(1)-C(2)-N(2b)	121.6	121.7	118.6	118.8	—	—
C(1)-C(2)-O(bs)	—	—	105.4	105.8	118.9	119.1
N(2a)-C(2)-N(2b)	116.9	116.7	114.1	113.9	—	—
N(2a)-C(2)-O(bs)	—	—	122.6	121.4	117.2	117.2
N(2b)-C(2)-O(bs)	—	—	47.5	47.3	—	—
C(1)-N(1a)-H(aa)	120.1	120.0	119.6	119.4	119.5	119.5
C(1)-N(1a)-H(as)	116.4	117.1	115.5	116.1	114.4	115.1
H(aa)-N(1a)-H(as)	121.8	121.3	120.7	120.2	120.6	120.2
C(1)-N(1b)-H(ba)	120.1	120.0	119.0	118.9	117.8	117.7
C(1)-N(1b)-H(bs)	116.4	117.1	117.8	118.2	115.6	115.6
H(ba)-N(1b)-H(bs)	121.8	121.3	117.8	117.5	115.4	115.3
C(2)-N(2a)-O(aa)	119.6	119.6	117.6	117.8	118.5	118.5
C(2)-N(2a)-O(as)	117.8	117.8	118.1	118.0	118.6	118.7
O(aa)-N(2a)-O(as)	122.6	122.6	124.3	124.2	123.0	122.8
C(2)-N(2b)-O(ba)	119.6	119.6	129.1	128.6	—	—
C(2)-N(2b)-O(bs)	117.7	117.8	76.1	76.1	—	—
O(ba)-N(2b)-O(bs)	122.6	122.6	119.7	119.4	109.7	109.5
C(2)-O(bs)-N(2b)	—	—	56.4	56.7	110.1	110.4
N(1a)-C(1)-C(2)-N(2a)c	-12.6	-12.6	11.4	12.4	6.2	6.1
N(1a)-C(1)-C(2)-N(2b)	167.4	167.4	-148.7	-149.0	—	—
N(1a)-C(1)-C(2)-O(bs)	—	—	161.7	161.5	-172.6	-172.7
N(1b)-C(1)-C(2)-N(2a)	167.4	167.4	-174.4	-173.2	-174.3	-174.5
N(1b)-C(1)-C(2)-N(2b)	-12.7	-12.6	25.4	25.4	—	—
N(1b)-C(1)-C(2)-O(bs)	—	—	-24.2	-24.1	6.9	6.8
C(1)-C(2)-N(2a)-O(aa)	-156.1	-154.8	178.6	177.0	175.6	175.4
C(1)-C(2)-N(2a)-O(as)	21.8	22.8	-0.8	-2.6	-4.1	-4.3
N(2b)-C(2)-N(2a)-O(aa)	24.0	25.2	-20.5	-20.8	—	—
N(2b)-C(2)-N(2a)-O(as)	-158.3	-157.2	160.2	159.6	—	—
O(bs)-C(2)-N(2a)-O(aa)	—	—	33.2	32.4	-5.6	-5.8
O(bs)-C(2)-N(2a)-O(as)	—	—	-146.2	-147.2	174.7	174.5
C(1)-C(2)-N(2b)-O(ba)	-155.9	-154.8	32.2	31.6	—	—
C(1)-C(2)-N(2b)-O(bs)	21.8	22.8	-84.9	-85.1	—	—
N(2a)-C(2)-N(2b)-O(ba)	24.0	25.2	-129.9	-131.8	—	—
N(2a)-C(2)-N(2b)-O(bs)	-158.3	-157.2	113.0	111.5	—	—
O(bs)-C(2)-N(2b)-O(ba)	—	—	117.1	116.8	—	—
C(1)-C(2)-O(bs)-N(2b)	—	—	114.9	114.9	-107.1	-106.4
N(2a)-C(2)-O(bs)-N(2b)	—	—	-94.1	-94.7	74.0	74.8
O(ba)-N(2b)-O(bs)-C(2)	—	—	-127.3	-126.7	-171.6	-170.9

a bond distances, b bond angles, c dihedral angles

TABLE 3: Selected Structural Parameters for Species 4−6

4, C_s [5]†, C_s 6, C_s

Geometrical Parameter	4 B3P86	4 B3LYP	5 B3P86	5 B3LYP	6 B3P86	6 B3LYP
C(1)-C(2)a	1.457	1.460	1.495	1.501	1.505	1.515
C(1)-N(1a)	1.331	1.336	1.301	1.305	1.293	1.294
C(1)-N(1b)	1.338	1.344	1.338	1.342	1.343	1.350
C(2)-N(2a)	1.452	1.462	1.416	1.423	1.413	1.420
C(2)-O(bs)	1.241	1.244	1.230	1.233	1.225	1.226
N(1a)-H(aa)	1.007	1.009	1.013	1.014	1.016	1.018
N(1a)-H(as)	1.023	1.021	1.277	1.264	*1.465*	*1.535*
N(1b)-H(ba)	1.006	1.007	1.006	1.007	1.006	1.007
N(1b)-H(bs)	1.013	1.013	1.012	1.013	1.012	1.012
H(as)-O(as)	*1.776*	*1.814*	1.180	1.203	1.059	1.038
N(2a)-O(aa)	1.221	1.227	1.225	1.232	1.226	1.233
N(2a)-O(as)	1.260	1.267	1.326	1.336	1.350	1.370
C(2)-C(1)-N(1a)b	124.9	125.19	119.3	119.2	119.6	119.8
C(2)-C(1)-N(1b)	113.3	113.75	112.7	113.2	111.6	111.7
N(1a)-C(1)-N(1b)	121.7	121.06	128.1	127.6	128.8	128.5
C(1)-C(2)-N(2a)	119.1	119.25	117.4	117.3	118.2	118.5
C(1)-C(2)-O(bs)	120.1	120.18	120.9	120.9	121.1	121.1
N(2a)-C(2)-O(bs)	120.8	120.57	121.7	121.8	120.8	120.4
C(1)-N(1a)-H(aa)	122.2	122.05	119.2	119.5	116.5	115.9
C(1)-N(1a)-H(as)	114.7	115.28	103.8	104.4	102.2	102.3
H(aa)-N(1a)-H(as)	123.1	122.48	137.1	136.1	141.4	141.8
C(1)-N(1b)-H(ba)	123.3	123.07	122.6	122.4	122.1	121.7
C(1)-N(1b)-H(bs)	115.7	116.32	116.8	117.3	117.5	118.2
H(ba)-N(1b)-H(bs)	121.0	120.61	120.6	120.3	120.4	120.1
N(1a)-H(as)-O(as)	—	—	154.9	154.5	154.5	153.3
C(2)-N(2a)-O(aa)	117.6	117.68	120.6	120.6	121.4	121.6
C(2)-N(2a)-O(as)	118.8	118.91	119.5	119.5	120.4	121.0
O(aa)-N(2a)-O(as)	123.5	123.42	119.9	119.9	118.2	117.5
H(as)-O(as)-N(2a)	—	—	105.2	105.1	105.1	105.2

a bond distances, b bond angles

decomposition process. Table 5 displays the relative (to DADNE) energies at every step during the decomposition of DADNE. Finally, Figure 2 depicts the reaction diagram.

Isonitrite, 3. Energetically, this species lies lower than DADNE by some 1.2 and 4.5 kcal/mol as calculated with the B3P86 and B3LYP methods, respectively. It is, however, highly unstable, since it immediately loses an NO radical via the Obs−N2b bond dissociation. The BDE obtained with B3P86 is 0.5 kcal/mol as compared to the negative B3LYP value of −6.6 kcal/mol for this reaction. Obviously, the error of this calculation is quite substantial. It is interesting to note that the analogous process for nitroethylene requires some 18.2 kcal/mol as calculated with B3P86 and 13.6 kcal/mol as calculated with B3LYP.[17] The G2 method gives an even higher value of 23.3 kcal/mol.[18] As with the C−NO2 BDE for DADNE, we expect that the DFT values are underestimated for this process too. Our rough prediction by comparison to nitroethylene would be a BDE of ~4−5 kcal/mol.

Hydrogen Atom Migration from NH$_2$ to NO$_2$. The remaining radical, **4**, (see Table 3) has a C−C bond length of 1.460 Å, as compared to 1.428 Å in **1**, as well as a C−NH$_2$ bond length (C1−N1a bond in Table 3) at 1.336 Å versus 1.345 Å in **1**. It is possible for the hydrogen atom, Has, to readily migrate from the NH$_2$ group to the NO$_2$ group, because the transition state, [**5**]†, of this reaction lies only 2.3 and 3.1 kcal/mol above **4** as calculated with B3P86 and B3LYP, respectively. The optimized geometrical parameters for the radical **4**, the transition state structure, [**5**]†, and the isomeric product, **6**, are shown in Table 3. All of these structures are planar. Product, **6**, lies energetically higher than the transition state, [**5**]†, if the ZPVE correction is made when calculating the differences in energy. If no ZPVE correction is made, **6** lies lower than [**5**]† by 0.4
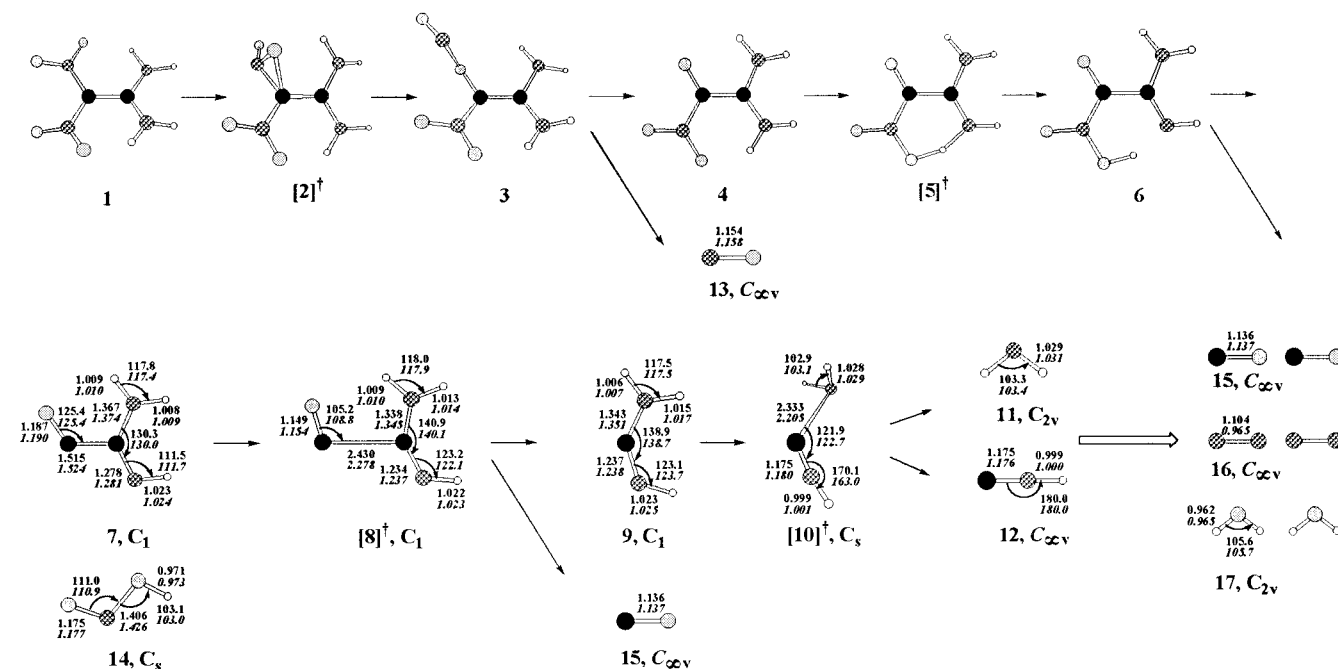
Figure 1. A scheme of unimolecular DADNE decomposition via the nitro-to-nitrite rearrangement pathway. The optimized geometrical parameters of species **1**–**3** and **4**–**6** are displayed in Tables 2 and 3, respectively. The regular and italic fonts indicate the use of the B3P86/6-31+G(d,p) and the B3LYP/6-31+G(d,p) methods, respectively.

TABLE 4: Absolute Energies, Imaginary Frequencies, and Zero-Point Vibrational Energies of All Chemical Species Involved in DADNE Decomposition via Nitro-to-Nitrite Pathway

structure	multiplicity, 2S+1	B3P86/6-31+G(d,p)			B3LYP/6-31+G(d,p)		
		energy, a.u.	ν_i, cm^{-1}	ZPVE, kcal/mol	energy, a.u.	ν_i, cm^{-1}	ZPVE, kcal/mol
1	singlet	−599.70979		58.23	−598.35631		57.68
[2]† ^{a}	singlet	−599.61090	811i	55.79	−598.25833	811i	55.20
3	singlet	−599.70961		56.85	−598.36127		56.25
13	singlet	−130.15256		2.88	−129.89548		2.83
4	doublet	−469.54989		51.17	−468.46495		50.71
[5]†	doublet	−469.54251	882i	48.80	−468.45647	1074i	48.30
6	doublet	−469.54317		50.54	−468.45832		50.34
14	singlet	−206.13464		12.91	−205.71501		12.69
7	doublet	−263.34187		34.52	−262.68909		34.29
[8]†	doublet	−263.31015	115i	30.89	−262.66246	198i	30.87
15	singlet	−113.55453		3.17	−113.31732		3.15
9	doublet	−149.75584		26.72	−149.34789		26.67
[10]†	doublet	−149.69465	131i	23.80	−149.29469	236i	23.94
11	doublet	−56.04295		12.01	−55.88545		11.91
12	singlet	−93.64976		9.22	−93.40924		9.17
16	singlet	−109.76926		3.54	−109.52978		3.51
17	singlet	−76.61055		13.49	−76.43405		13.36

^{a} Symbols such as [2]† refer to a transition state.

and 1.1 kcal/mol as calculated with B3P86 and B3LYP, respectively. This indicates that the calculations are not accurate. However, we may conclude that the differences in energy between species **4**–**6** are small and that **4** may easily be converted to **6** and vice versa.

HONO Elimination. We considered several possibilities of species **4** and **6** decomposition on a doublet potential energy surface (PES). Species **4** could undergo either NO$_2$ or NH$_2$ radical elimination, while species **6** could undergo NH$_2$ radical or HONO molecule elimination. However, only the HONO elimination from **6** would result in the formation of a reasonably stable conjugated structure, radical **7**. We were not able to locate the transition state for HONO elimination from **6**. We thus obtained a PES by optimizing the geometry at a series of fixed C2−N2a bond lengths in **6**. The energy of the system increases with an increasing bond length at first and then reaches a plateau.

Therefore, the barrier for this process is approximately equal to the differences in energy between the reactant, **6**, and the two products, **7** and **14**. We calculated this barrier to be 38.7 and 25.1 kcal/mol with the use of B3P86 and B3LYP, respectively.

The large difference between the values for this barrier obtained from the two methods merits a comment. While investigating the decomposition of nitroethylene,[18] we found that the results obtained from the use of B3P86 and B3LYP were similar in almost all of the steps, except the ones which result in HONO formation. Moreover, the B3LYP results come reasonably close to the G2 results, while the B3P86 results are overestimations as compared to the results obtained from the G2 method. Comparison of optimized geometrical parameters with the experimental ones also indicates that the B3LYP calculations are preferable. The experimental HO−N bond
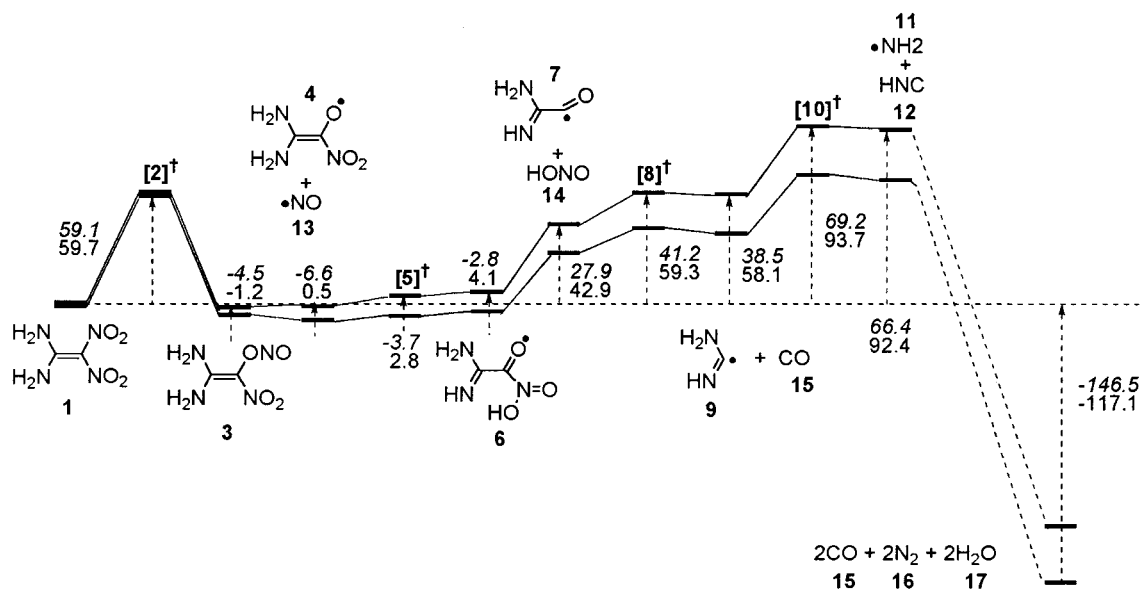
Figure 2. The energetic profile of DADNE decomposition via the nitro-to-nitrite rearrangement pathway. All of the energies are in reference to DADNE. The units are kcal/mol. The regular and italic fonts indicate the use of the B3P86/6-31+G(d,p) and the B3LYP/6-31+G(d,p) methods, respectively.

TABLE 5: Relative (to DADNE) Energies in kcal/mol at Every Step of DADNE Decomposition via Nitro-to-Nitrite Pathway

	B3P86			B3LYP		
structure	uncorrected for ZPVE	corrected for unscaled ZPVE	corrected for scaled ZPVE	uncorrected for ZPVE	corrected for unscaled ZPVE	corrected for scaled ZPVE
[2]†	62.1	59.6	59.7	61.5	59.0	59.1
3	0.1	−1.3	−1.2	−3.1	−4.5	−4.5
4+13	4.6	0.4	0.5	−2.6	−6.7	−6.6
[5]†+13	9.2	2.7	2.8	2.7	−3.8	−3.7
6+13	8.8	4.0	4.1	1.6	−2.9	−2.8
7+14+13	50.7	42.7	42.9	35.6	27.7	27.9
[8]†+14+13	70.6	59.0	59.3	52.3	41.0	41.2
9+15+14+13	70.4	57.8	58.1	50.6	38.3	38.5
[10]†+15+14+13	108.8	93.4	93.7	84.0	68.9	69.2
11+12+15+14+13	110.0	92.0	92.4	84.0	66.0	66.4
15×2+16×2+17×2	−99.7	−117.5	−117.1	−129.3	−146.9	−146.5

length is 1.433 Å versus 1.426 Å and 1.406 Å as calculated with B3LYP and B3P86, respectively. Thus, the B3LYP result appears to be somewhat more trustworthy here. Additional information on the performance of DFT methods, including the comparison of experimental and calculated geometrical parameters for the HONO system, can be found in a recent work by Jursic.[27]

CO Elimination. The C−C bond appears to be the weakest spot in structure **7**. CO elimination may occur on a doublet PES with a barrier of only 16.4 and 13.3 kcal/mol as calculated with B3P86 and B3LYP, respectively. The transition state, [**8**]†, has an extremely long C−C distance of 2.278 Å and one imaginary frequency of 198i. The products of this reaction are the radical, **9**, and CO, **15**, which is an extremely stable molecule.

NH$_2$ Radical Elimination. The remaining fragment, **9**, may further decompose into NH$_2$ radical, **11**, and HNC, **12**, via NH$_2$ radical elimination on a doublet PES. The barrier is 35.6 and 30.7 kcal/mol as calculated with B3P86 and B3LYP, respectively. The transition state, [**10**]†, has a long C−NH$_2$ distance of 2.205 Å and one imaginary frequency of 236i.

Final Stages of DADNE Decomposition. So far we showed how unimolecular decomposition of DADNE may lead to the formation of the following fragments: NO radical, HONO, CO, NH$_2$ radical, and HNC. Clearly, these fragments may undergo collisions and thus react with other fragments and with yet un-

reacted molecules. The number of possibilities is large. We point out below, however, some of the most important and the most likely reactions to occur in the final stages of DADNE decomposition. They all have rather low activation energies (determined either experimentally and/or theoretically by various authors, see refs 27−30) and lead to stable products, N$_2$, CO, and H$_2$O.

(a)[27] $HONO \rightarrow \bullet NO + \bullet OH$

(b)[28] $\bullet NO + \bullet NH_2 \rightarrow N_2 + H_2O$

(c)[29] $HNC + \bullet OH \rightarrow \bullet CN + H_2O$

(d)[29] $HNC \rightarrow HCN$

(e)[29] $HCN + \bullet OH \rightarrow \bullet CN + H_2O$

(f)[30] $\bullet CN + \bullet NO \rightarrow N_2 + CO$

The two N$_2$, two CO, and two H$_2$O molecules energetically lie below DADNE by an impressive 117.1 and 146.5 kcal/mol as obtained with B3P86 and B3LYP, respectively.

Additional Check on the Accuracy of DFT Calculations

As mentioned earlier, we calibrated our use of the DFT methodology, applied in this paper, by comparing DFT results

TABLE 6: Single Point MP2 Energies Calculated at the B3LYP/6-31+G(d,p) Optimized Geometries for the Initial Step of DADNE Decomposition, along the Nitro-to-nitrite Reaction Pathway[a]

	MP2/6-31G(d,p) I	MP2/6-311+G(d,p) II		E_a, kcal/mol	
structure	energy, a.u.	energy, a.u.	method of E_a calculation	I	II
1	−596.73483	−597.02531	uncorrected for ZPVE	59.4	58.4
[2]†	−596.64021	−596.93230	corrected for unscaled ZPVE	56.9	55.9
3	−596.73662	−597.02909	corrected for scaled ZPVE	56.9	55.9

[a] For two different basis sets, 6-31G(d,p) (I) and (6-311+G(d,p) (II), the energies are listed for structures **1** (DADNE), [**2**]† (transition state), and **3** (isonitrite). The activation energy, E_a, is listed for both basis sets I and II. The ZPVE corrections used were obtained from the B3LYP/6-31+G(d,p) calculations.

with ab initio results (MP2, MP4, G2) for the related molecule, nitroethylene. However, for purposes of having one additional check on the accuracy of DFT as applied to DADNE, and at the same time obtaining additional information concerning the first step of particular interest in the decomposition, we have carried out ab initio MP2 calculations on the structures **1**, [**2**]†, and **3**, which define the first step in the nitro-to-nitrite rearrangement reaction pathway. The energy values calculated by the MP2 method with two different basis sets, viz., 6-31G(d,p) (I) and 6-311+G(d,p) (II), at the B3LYP geometries, for these three structures are listed in Table 6. Recall that our DFT prediction for the crucial initial step in the nitro-to-nitrite rearrangement pathway was an activation energy of 59.7 and 59.1 kcal/mol, obtained with the B3P86 and B3LYP methods, respectively. This prediction is very close to and just above the experimental activation energy of 58 kcal/mol. In Table 6 we list the MP2 predictions for the same activation energy obtaining 56.9 and 55.9 kcal/mol with basis sets I and II, respectively, very close to and just below the experimental value. Thus, the assumed errors in the DFT methodology are not expected to change the conclusions associated with our calculated DFT results. The closeness of DFT to MP2 predictions of the activation energy lends support to the use of DFT calculations in this study.

Concluding Remarks

In this paper the calculations made and the conclusions drawn are based on DFT methodology. While there are errors to be expected in applying DFT calculations to the various steps in the reaction path studied, we have relied upon our experience[18] with the simpler but related molecule nitroethylene to help characterize the magnitude of the errors. In the simpler case we made both ab initio (MP2, MP4, and G2) and DFT calculations. We used the simpler molecule to estimate the level of basis that would be adequate for reliable results. In that way, we chose the basis sets used here for DADNE. In those steps that are similar in both molecules, for example, the critical nitro-to-nitrite rearrangement, the errors associated with DFT, judged against the ab initio results as standard, were likely to be similar in both molecules. This permitted us to use relatively efficient DFT calculations to characterize the unimolecular decomposition of DADNE.

We have found that the initial step in the unimolecular decomposition of DADNE is a nitro-to-nitrite rearrangement. The calculated barrier to transition at 59.1 kcal/mol B3LYP (59.7 kcal/mol B3P86) compares very well with the experimental value of 58 kcal/mol, and with the single-point MP2 calculations (see Table 6) performed at the B3LYP optimized geometry. Once the initial barrier is surmounted, the decomposition proceeds through a series of steps, all of which we were able to characterize, involving relatively low energy barriers, resulting in the production of fragments NO, HONO, CO, NH_2, and HNC.

We pointed out how these fragments may plausibly interact to yield, as final stable products, CO, N_2, and H_2O. These final products lie below the original DADNE molecule by 146.5 kcal/mol B3LYP (117.1 kcal/mol B3P86). On average, the energy released by one DADNE molecule is sufficient to activate two additional molecules, and thus a chain reaction may be sustained.

The structural parameters that we have calculated for DADNE are consistent with the experimental crystallographic structure,[2,3] and also with the previous calculations of Politzer et al.[4] Additionally, we have obtained the structural parameters for the initial transition state, as well as for each subsequent step along the decomposition pathway. Thus, the unimolecular decomposition of DADNE appears to be well characterized.

Supporting Information Available: Table of calculated values of the vibrational frequencies for each structure. This material is available free of charge via the Internet at http://pubs.acs.org.

References and Notes

(1) Latypov, N. V.; Bergman, J.; Langlet, A.; Wellmar, U.; Bemm, U. *Tetrahedron* **1998**, *54,* 11525.

(2) Bemm, U.; Östmark, H. *Acta Crystallogr.* **1998**, *C54,* 1997.

(3) Gilardi, R. Crystallographic data (excluding structure factors) for the DADNE structure have been deposited with the Cambridge Crystallographic Data Centre, 12 Union Road, Cambridge CB2 1EZ, U.K. (deposition number CCDC 127539).

(4) Östmark, H.; Langlet, A.; Bergman, H.; Wingborg, U.; Wellmar, U.; Bemm, U. FOX-7 − A New Explosive with Low Sensitivity And High Performance; *11th International Symposium on Detonation*, 1998; http://www.sainc.com/onr/detsymp/financcmt.html.

(5) Politzer, P.; Concha, M. C.; Grice, M. E.; Murray, J. S.; Lane, P. *J. Mol. Struct. (THEOCHEM)* **1998**, *452,* 75. Also refs 1 and 2 therein.

(6) Zhao, X.; Hintsa, E. J.; Lee, Y. T. *J. Chem. Phys.* **1988**, *88,* 801.

(7) Shalashilin, D. V.; Thompson, D. L. *J. Phys. Chem. A* **1997**, *101,* 961.

(8) Wu, C. J.; Fried, L. E. *J. Phys. Chem. A* **1997**, *101,* 8675.

(9) Lofy, P.; Wight, C. A. Thermal Decomposition of HMX (Octahydro-1,3,5,7-tetranitro-1,3,5,7-tetrazocine) Below its Melting Point; *Proceedings of the JANNAF Combustion and Hazards Meeting*, Tucson, Arizona, 1998.

(10) Rice, B. M.; Chabalowski, C. F. *J. Phys. Chem. A* **1997**, *101,* 8720.

(11) Melius, C. F. Thermochemical Modeling: I. Application to Decomposition of Energetic Materials. In *Chemistry and Physics of Energetic Materials*; Bulusu, S. N., Ed.; Kluwer Academic Publishers: The Netherlands, 1990; Vol. 301, pp 21−49.

1,1-Diamino-Dinitroethylene Decomposition

J. Phys. Chem. A, Vol. 103, No. 50, 1999 **11051**

(12) Melius, C. F. Thermochemical Modeling: II. Application to Ignition and Combustion of Energetic Materials. In *Chemistry and Physics of Energetic Materials*; Bulusu, S. N., Ed.; Kluwer Academic Publishers: The Netherlands, 1990; Vol. 301, pp 51−78.

(13) Behrens, R., Jr. *J. Phys. Chem.* **1990**, *94,* 6707.

(14) Behrens, R., Jr.; Bulusu, S. *J. Phys. Chem.* **1991**, *95,* 5838.

(15) Behrens, R., Jr.; Bulusu, S. *J. Phys. Chem.* **1992**, *96,* 8877.

(16) Behrens, R., Jr.; Bulusu, S. *J. Phys. Chem.* **1992**, *96,* 8891.

(17) Behrens, R., Jr.; Mack, S.; Wood, J. Thermal Decomposition Mechanisms of HMX: The Interrelationship of Chemical and Physical Processes. *Proceedings of the JANNAF Combustion and Hazards Meeting*, Tucson, Arizona, 1998.

(18) Gindulytė, A.; Massa, L.; Huang, L.; Karle, J. *J. Phys. Chem. A* **1999**, *103*, XXXXX.

(19) Hu, C.-H.; Chong, D. P. Density Functional Applications. In *Encyclopedia of Computational Chemistry*; Schleyer, P. v. R., Allinger, N. L., Clark, T., Gasteiger, J., Kollman, P. A., Schaefer, H. F., III, Schreiner, P. R., Eds.; John Wiley & Sons: New York, 1998; pp 664−678.

(20) Frisch, M. J.; Trucks, G. W.; Schlegel, H. B.; Scuseria, G. E.; Robb, M. A.; Cheeseman, J. R.; Zakrzewski, V. G.; Montgomery, J. A., Jr.; Stratmann, R. E.; Burant, J. C.; Dapprich, S.; Millam, J. M.; Daniels, A. D.; Kudin, K. N.; Strain, M. C.; Farkas, O.; Tomasi, J.; Barone, V.; Cossi, M.; Cammi, R.; Mennucci, B.; Pomelli, C.; Adamo, C.; Clifford, S.; Ochterski, J.; Petersson, G. A.; Ayala, P. Y.; Cui, Q.; Morokuma, K.; Malick, D. K.; Rabuck, A. D.; Raghavachari, K.; Foresman, J. B.; Cioslowski, J.; Ortiz, J. V.; Stefanov, B. B.; Liu, G.; Liashenko, A.; Piskorz, P.; Komaromi, I.; Gomperts, R.; Martin, R. L.; Fox, D. J.; Keith, T.; Al-Laham, M. A.; Peng, C. Y.; Nanayakkara, A.; Gonzalez, C.; Challacombe, M.; Gill, P. M. W.; Johnson, B.; Chen, W.; Wong, M. W.; Andres, J. L.; Gonzalez, C.; Head-Gordon, M.; Replogle, E. S.; Pople, J. A. *Gaussian 98*, Revision A.6; Gaussian, Inc.: Pittsburgh, PA, 1998.

(21) Foresman, J. B.; Frisch, A. *Exploring Chemistry with Electronic Structure Methods,* 2nd ed.; Gaussian, Inc.: Pittsburgh, 1996.

(22) Becke, A. D. *J. Chem. Phys.* **1993**, *98,* 5648.

(23) Perdew, J. P. *Phys. Rev. B* **1986**, *33,* 8822.

(24) Lee, C.; Yang, W.; Parr, R. G. *Phys. Rev. B* **1988**, *37,* 785.

(25) Scott A. P.; Radom L. *J. Phys. Chem.* **1996**, *100*, 16502.

(26) Guirguis, R.; Hsu, D.; Bogan, D.; Oran, E. *Combust. Flame* **1985**, *61,* 51.

(27) Jursic, B. S. *Chem. Phys. Lett.* **1999**, *299,* 334.

(28) Wolf, M.; Yang D. L.; Durant, J. L. *J. Phys. Chem.* A **1997**, *101*, 6243.

(29) Palma, A.; Semprini, E.; Stefani, F.; Talamo, A. *J. Chem. Phys.* **1996**, *105*, 5091.

(30) Klippenstein, S. J.; Yang, D. L.; Yu, T.; Kristyan, S.; Lin, M. C.; Robertson, S. H. *J. Phys. Chem. A* **1998**, *102*, 6973.